Communications on Applied Nonlinear Analysis
ISSN: 1074-133X
Vol 32 No. 9s (2025)

# Synthesis and Characterization of $CO_3O_4$ Nanoparticles Using Microwave-Assisted Method

**S Sumathy [a], Goparaju Savithri [b], M Mohanraj [c] and M Parthasarathy [a*]**

*[a,b,c] Department of Physics, School of Basic Sciences, Vels Institute of Science, Technology and Advanced Studies (VISTAS), Pallavaram, Chennai-600 117, Tamil Nādu, India.*

*** Corresponding author email: mps2k7@gmail.com (Dr. M. Parthasarathy)**

***Article History:***

***Received: 12-11-2024***

***Revised: 10-12-2024***

***Accepted: 15-01-2025***

**Abstract:**

Nanoscience primarily focuses on the synthesis, characterisation, exploration, and application of nanostructured materials, which are defined by having at least one dimension in the nanometer range. $CO_3O_4$ nanoparticles are exceptionally cost-effective and highly stable conductive materials featuring a broad bandgap. These nanoparticles are crucial for supercapacitor applications, and $CO_3O_4$ is regarded as one of the most promising positive anode materials. Cobalt oxide nanopowder has been successfully synthesized using the microwave method, allowing for better control over the production process. Characterisation techniques validated the structural properties of cobalt oxide through X-ray diffraction (XRD), which confirmed a face-centred cubic structure. Fourier-transform infrared (FT-IR) analysis revealed significant vibrational bands at 663.5 $cm^{-1}$ and 574.7 $cm^{-1}$, while impedance spectroscopy assessed electrical conductivity at elevated temperatures. Field-emission scanning electron microscopy (FE-SEM) showed a spherical morphology, and Energy-dispersive X-ray spectroscopy (EDAX) confirmed the presence of constituent elements. Additionally, high-temperature electrical resistivity measurements indicated a decrease in resistance with increased temperature. The maximum specific capacitance of 344 F/g was obtained from cyclic voltammetry (CV) studies.

**Keywords:** Microwave method, XRD, FT-IR, FE-SEM and Cyclic Voltammetry

## 1 Introduction

Microwave heating has emerged as a significant method for the synthesis of nanomaterials. Our research group and others in the field have employed microwave techniques for synthesising various transition metal oxides, including Cobalt, Nickel, Zinc and Silver Oxide. This method offers multiple advantages, such as uniform heating throughout the reaction vessel and the capacity for selective heating based on the specific properties of the materials involved. Our findings indicate that microwave synthesis effectively controls nanostructured materials' particle size distribution and macroscopic morphology [1][2]. Furthermore, this technique enables modifications to morphology and facilitates reduced crystallisation times, leading to improvements in the degree of silica condensation within the mesoporous walls during synthesis. In this investigation, microwave synthesis enhanced crystallisation conditions essential for developing mesoporous materials. Distinct from conventional heating practices, microwave processes generate heat directly through the interaction of molecules within the heated material induced by electromagnetic fields produced in the microwave apparatus.

This processing technique proves advantageous for materials possessing high dielectric constants, as the absorption of microwave energy is contingent upon the dielectric constants and loss factors of the substrates. Water, highly efficient in absorbing microwave energy, exemplifies this due to its substantial dielectric constant, particularly effective at the frequency of 2.450 GHz. Consequently, the microwave effect on the synthesis of $CO_3O_4$ is anticipated to be significantly amplified [3]. Our results demonstrate that this methodology serves as a potent tool for regulating the dimensions of nanoparticles. Cobalt oxide ($CO_3O_4$) nanoparticles exhibit distinctive properties and possess diverse applications across various fields. These nanoparticles are utilised in gas sensing and diverse anode materials for energy storage devices, magnetic materials, supercapacitors, field emission materials, magneto-resistive devices, and catalysis. Cobalt oxide is an anti-ferromagnetic material and a p-type semiconductor with advantageous properties for application in optical, electrochemical, and field emission devices [4][5].

## 2 Experimental Procedure

### 2.1 Materials and Methods

High-purity cobalt (II) nitrate hexahydrate and sodium hydroxide were used as the starting materials. 31.290 grams of Co (NO3)2·6H2O in water to make a 0.2 M and 8.602 grams of NaOH in water to 0.4 M. The NaOH solution was gradually added to the $Co(NO_3)_2{\cdot}6H_2O$ solution, drop by drop, while continuously stirring at room temperature until the pH reached 12. The reaction proceeds as follows:

$$\mathbf{Co\,(No_3)_2.6H_2O + 2NaOH + H_2O \rightarrow Co\,(OH)_2\downarrow + 2NaNO_3 + 7H_2O}$$

The above precipitate solution was reheated in a microwave oven at 500W for 8 min. A grey-coloured precipitate was rapidly produced and then filtered [6]. It was then washed many times using deionised water until the pH was 7, dried in the air, and annealed in an air atmosphere at 300°C / 1 hr, 300°C / 2 h, and 300°C / 3 h, respectively, to get a dark-coloured Nanocrystalline $Co_3O_4$ powder.

## 3 OUTCOMES AND ANALYSIS

### 3.1. XRD Analysis

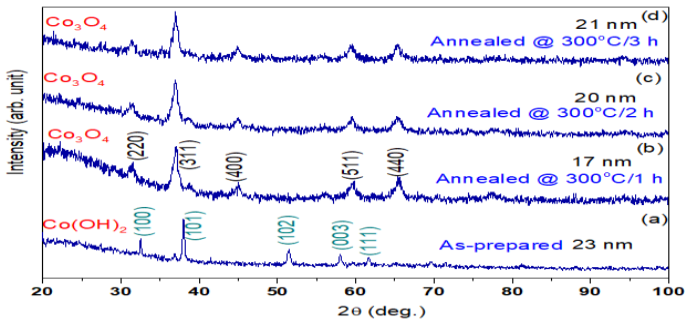


**Figure. 1 XRD patterns of nanocrystalline $Co_3O_4$ (a) as-prepared, annealed at (b) 300 °C for 1 h, (c) 300 °C for 2 h and (d) 300 °C for 3 h**

Figure 1(a) shows the XRD peaks of the as-prepared β–Co(OH)2 sample, revealing five distinctive peaks indicative of nanocrystalline pure Co(OH)2, which features a hexagonal structure (JCPDS# 30-0443). In contrast, XRD patterns Figure 1(b) present the β–Co(OH)2 that underwent annealing at 300 ºC in the air for one hour. This spectrum displays five prominent diffraction peaks at 2θ values of 31.52º, 37.07º, 45.14º, 59.62º, and 65.55º. These peaks correspond to the (2 2 0), (3 1 1), (4 0 0), (5 1 1), and (4 4 0) planes of Co3O4, as referenced in JCPDS # 074-1657. The XRD patterns suggest a face-centred cubic structure [7]. Using the Scherrer formula,

$$t = 0.9\,\lambda / \beta \cos \theta_B$$

The average crystalline size of nanocrystalline $CO_3O_4$ was found to be 17 nm. As illustrated in Figure 1(c), β–Co(OH)2, annealed at 300 ºC for 2 hours, displays crystal planes characteristic of Co3O4, with five prominent peaks observed at approximately 31.44º, 36.93º, 45.01º, 59.61º, and 65.44º [8]. The average crystalline size for this specific sample of nanocrystalline Co3O4 was measured to be 20 nm. Furthermore, Figure 1(d) reveals that β–Co(OH)2, subjected to annealing at 300 ºC for 3 hours, exhibited the largest crystalline size of 21 nm compared to the other analysed samples. This increase in size may be attributed to greater energy availability, facilitating enhanced crystal growth as the duration of annealing is prolonged.

### 3.2. FT-IR Spectral Analysis

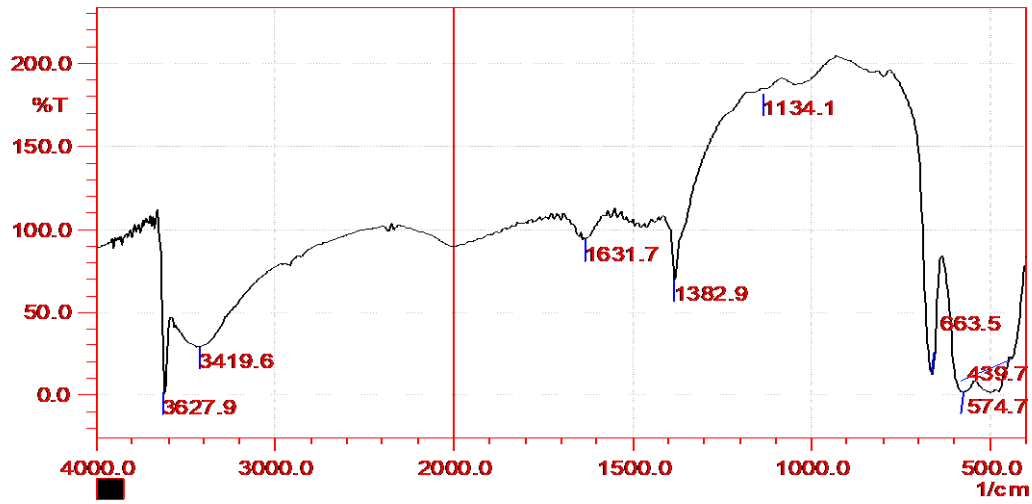


**Figure. 2 FT-IR Spectrum of the $Co(OH)_2$ as prepared sample**

The FT-IR spectra were recorded in the 4000 $cm^{-1}$ to 400 $cm^{-1}$ using a Bruker 66V spectrometer. As illustrated in Figure 2, the FT-IR spectrum of the synthesised cobalt hydroxide, $Co(OH)_2$, along with the nanocrystalline $Co(OH)_2$ sample, reveals a broad absorption band centred at 3419.6 $cm^{-1}$. The peak at 1631.7 $cm^{-1}$ is attributed to water's O-H stretching and bending modes. Additionally, the sharp peak at 3627.9 $cm^{-1}$ signifies the presence of free hydroxyl groups. The distinct peak at 1382.9 $cm^{-1}$ corresponds to the bending vibrations of absorbed $CO_2$ or $CH_2$. Regarding the $CO_3O_4$ nanoparticles, the absorption bands at 574.7 $cm^{-1}$ and 663.5 $cm^{-1}$ are indicative of Co(III)–O and Co(II)–O stretching vibrations, respectively, thereby confirming the formation of the $CO_3O_4$ spinel oxide phase [9].

### 3.3 IMPEDANCE SPECTROSCOPY MEASUREMENTS

**(Complex impedance plot of nanocrystalline $Co_3O_4$)**

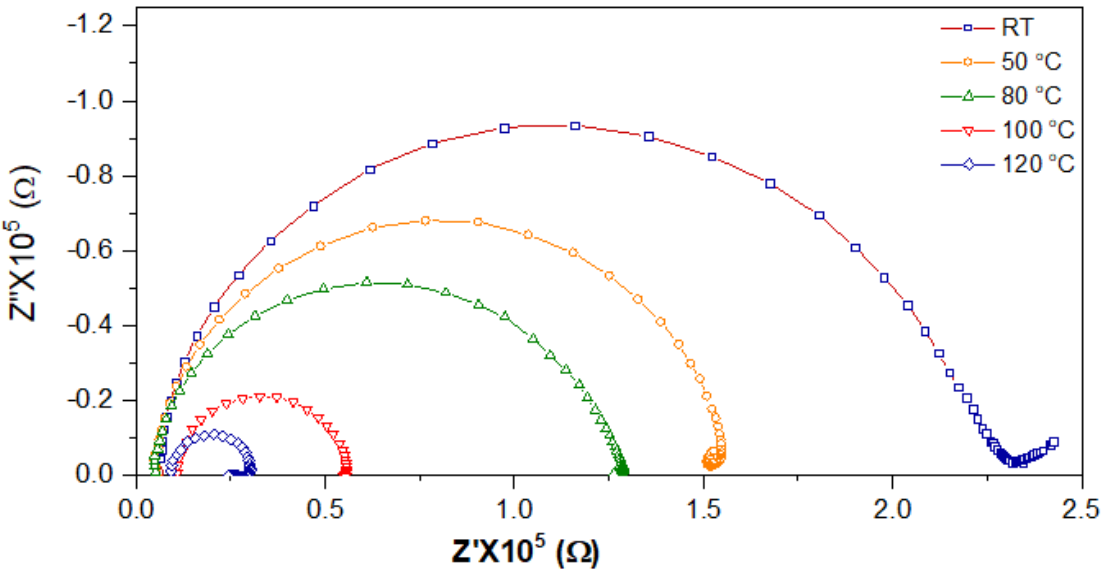


**Figure. 3(a) Impedance plots from RT to 120 ºC**

Complex impedance plots at room temperature to 120ºC, covering frequencies of 1 Hz to 10 MHz, are shown in Figure 3 (a). It is important to note that this plot reveals a single depressed semicircle, with its centre slightly displaced below the real axis. At lower temperatures and lower measuring frequencies, the curve exhibits deviations from an ideal semicircle [10]. Subsequently, this resistance value was calculated using the relation.

$$\sigma = 1/\rho = l/RA$$

Figure 3(b) shows a graph of nanocrystal Co3O4 ceramics. The activation energy is expressed as

$$\sigma_T = \sigma_0 \exp(-E_a / k_B T)$$

It is also observed that conductivity increases with temperature from room temperature to 140˚C. $Co_3O_4$ (a standard spinel-type structure) is a versatile semiconductor [11].

Conductivities for most stoichiometric transition element oxides are of the order of $10^{10}$ $\Omega^{-1}$ $cm^{-1}$ at room temperature. The plotted data (conductivity against temperature) in Figure 3(b) shows two activation energy values are obtained for the nanocrystalline $CO_3O_4$: one in a lower region between room temperature and 90˚C and another in a higher temperature region between 90 ˚C and 140 ˚C. The activation energies are measured at 0.15 eV and 0.74 eV, accordingly.

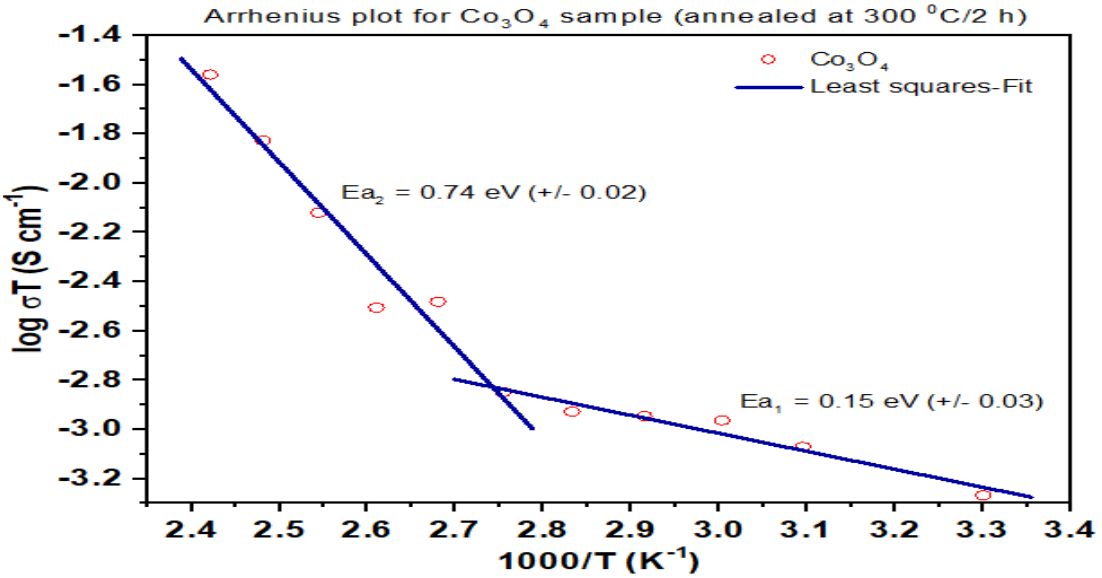


**Figure. 3(b) The activation energy for nanocrystalline $Co_3O_4$**

Figure 3(b) shows that only two straight lines are observed at RT – 90 ºC and 90 ºC - 140°C. The activation energies were 0.15 eV for the first stage (extrinsic) and 0.74 eV for the second stage (intrinsic). Detailed interpretation of activation energy is complicated for $Co_3O_4$ ceramic semiconductors with grains, grain boundaries and pores.

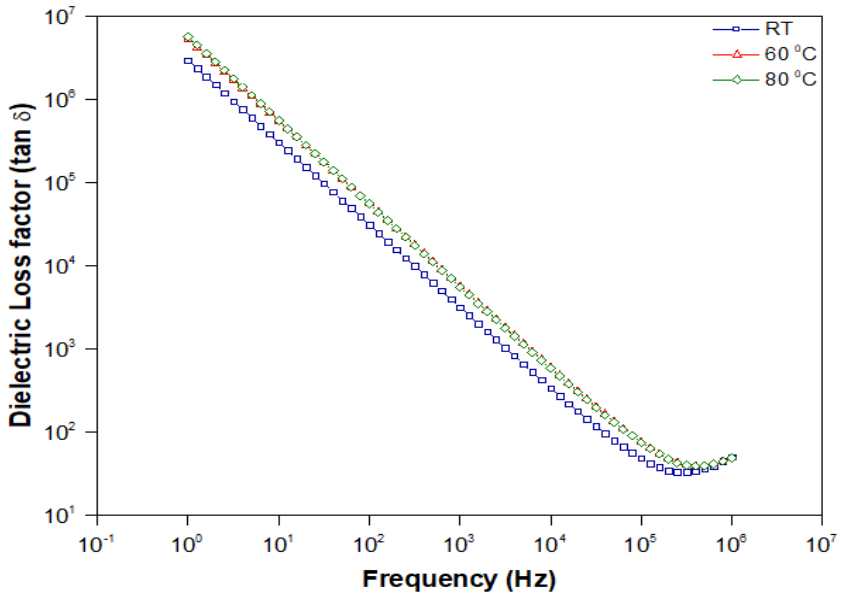


**Figure. 3(c) Frequency dependence of the dielectric constant of $Co_3O_4$**

Figure 3(c) shows how the dielectric constant changes with frequency at different temperatures. The dielectric constant becomes saturated at higher frequencies because the electronic exchange between Co2+ and Co3+ ions cannot keep up with the alternating current field, which extends beyond a specific frequency. From this measurement, the frequency of nanocrystalline $Co_3O_4$ increases, and the dielectric loss factor decreases for the same reason described in Figure 3(d).

### 3.4 High-Temperature Electrical Resistivity

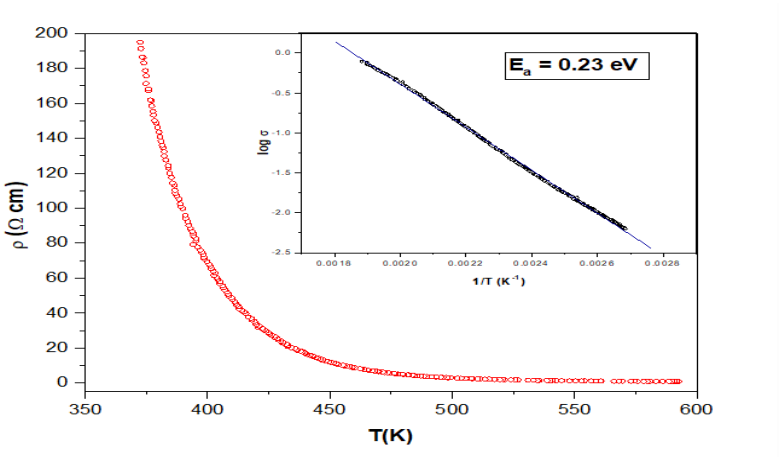


**Figure. 4 High-Temperature electrical resistivity plot of n-$Co_3O_4$**

Figure 4 presents the resistivity of $CO_3O_4$, measured at temperatures ranging from 350 K to 600 K. It was observed that the resistance of nanocrystalline $CO_3O_4$ decreases as the temperature increases within this range, demonstrating a negative temperature coefficient of resistance indicative of its semiconductor behaviour. This phenomenon, where the resistance of n-$CO_3O_4$ diminishes with rising temperature, is attributed to an activated mechanism [12]. The activation energy determined from the Arrhenius plot is Ea = 0.23 Ev

### 3.5 Field Emission Scanning Electron Microscopic Analysis (FE-SEM)

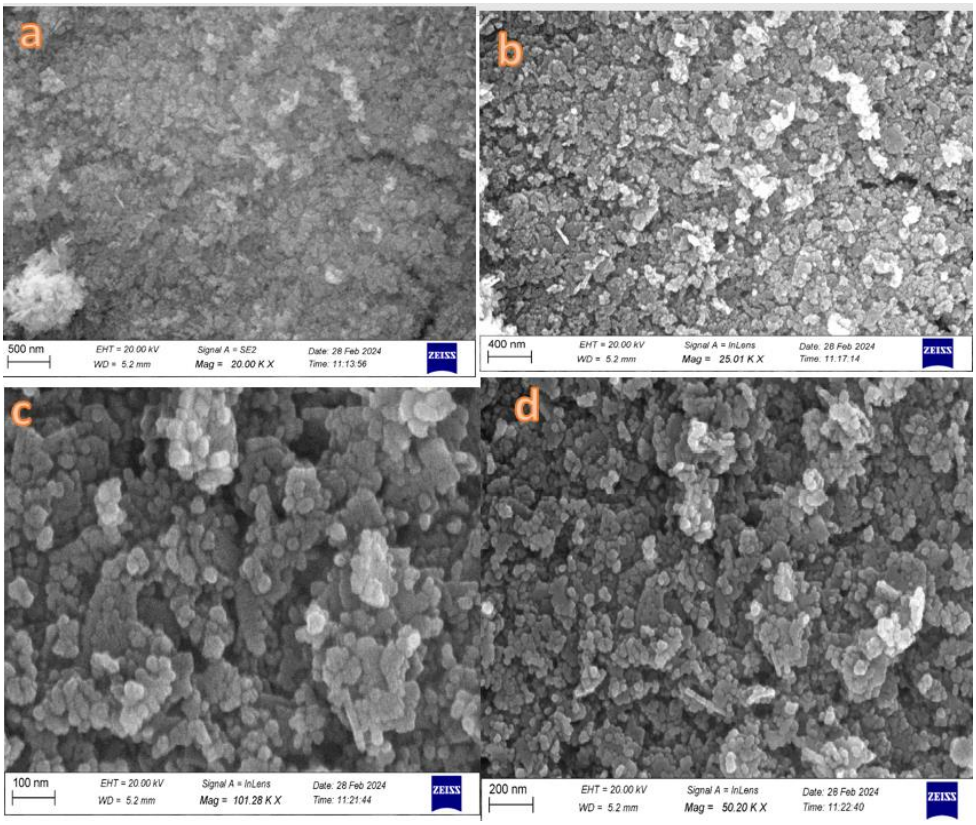


**Figure. 5 FE-SEM of $CO_3O_4$ Nanoparticles**

Figure. 5 shows the morphology of the synthesised $CO_3O_4$ nanoparticles, examining the interaction signals between electrons and the material, thereby providing insights into the quality of the nanostructure. The finely powdered crystalline sample was inspected by field emission spectroscopy (FE-SEM) at different magnifications of 100nm, 200nm, 400nm, and 500nm, as shown in Figure. 5. The magnified images revealed a distinctly defined atomic arrangement, indicating a sphere-like morphology structure. The image illustrates a cluster of particles, suggesting effective connectivity among the nanoparticles [13]. Field Emission Scanning Electron Microscopy (FE-SEM) offers insights into the dimensions of the nanoparticles. EDAX was conducted to evaluate the sample's composition. The EDAX spectrum is presented in Figure 6. It shows the presence of the constituent elements, affirming the material's high purity and quality is shown in Table 1.

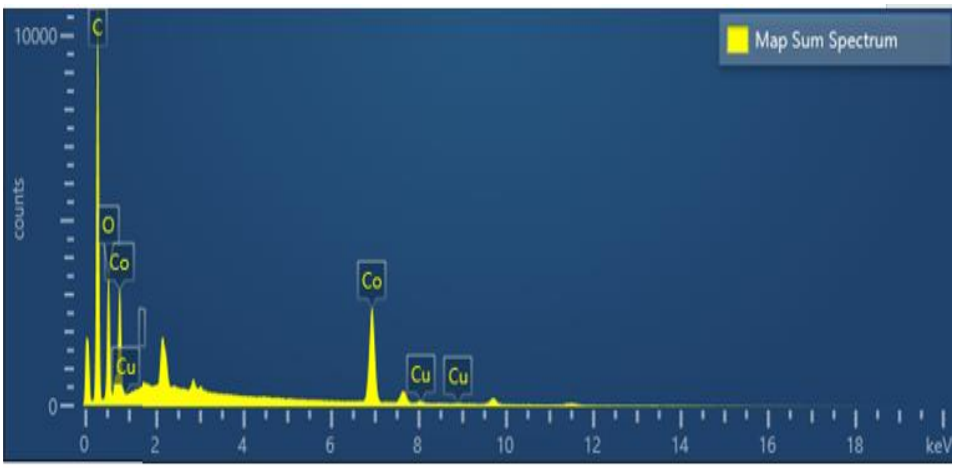


**Figure. 6 EDAX Spectrum of $CO_3O_4$**

| Map sum Spectrum | | | | |
|---|---|---|---|---|
| **Element** | **Line Type** | **Weight %** | **Weight % sigma** | **Atomic %** |
| C | K series | 63.57 | 0.23 | 77.16 |
| O | K series | 20.94 | 0.24 | 19.02 |
| CO | K series | 14.92 | 0.13 | 3.69 |
| Cu | K series | 0.57 | 0.07 | 0.13 |
| Total | | 100.00 | | 100.00 |

**Table 1. EDAX Map Sum Spectrum of $CO_3O_4$**

### 3.6 Cyclic Voltammetric (CV) studies

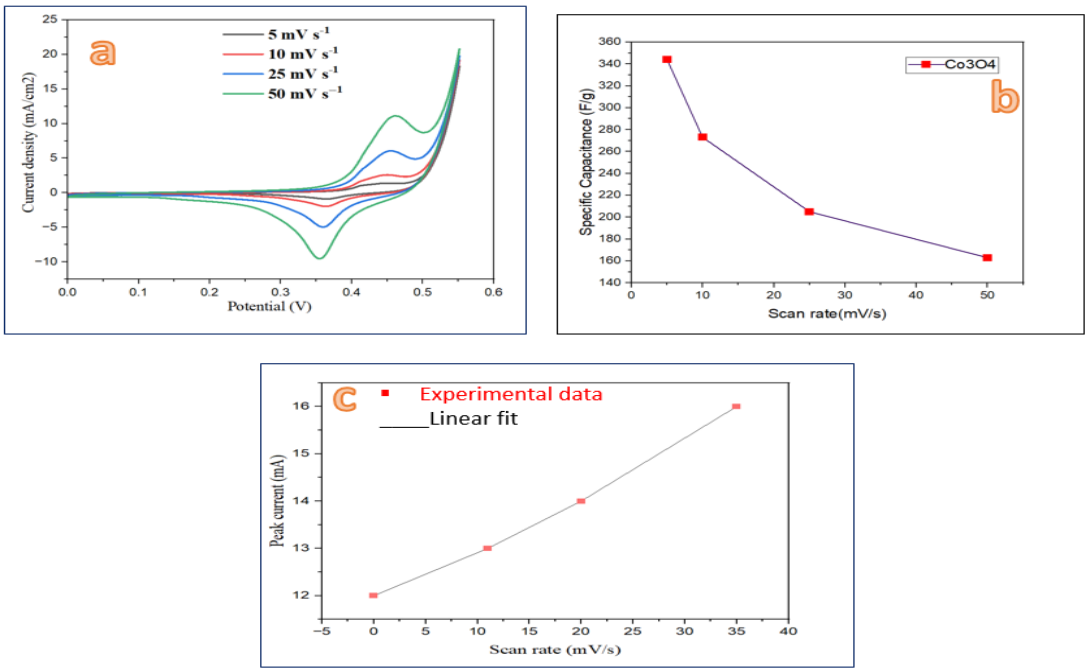


**Figure. 7 Cyclic Voltammetry Studies for $CO_3O_4$ (a) Current density**

**(b) Specific Capacitance (c) Peak current of electrode**

Figure. 7 shows the cyclic voltammogram of $Co_3O_4$ electrodes at different scan rates in the potential range of 0 to 0.5 V using 2.0 M KOH as the electrolyte. CV curve exhibits well-defined redox peaks, confirming the Faradic nature of the material rather than electric double-layer capacitor behaviour that is an ideal rectangular shape. In CV, the anodic and cathodic peaks are not symmetric due to kinetic irreversibility in the redox process. The shape of the CV curve changes while increasing the scan rate [14]. The anodic peaks shift towards significant anodic potential while increasing the scan rate. The anodic peaks shift towards significant anodic potential, and the cathodic peaks shift towards considerable cathodic potential with an increased scan rate. Figure 7(a) shows the variation of anodic peak current density with scan rate. This linearity of the peak current with scan rate suggests surface redox reactions leading to the pseudo-capacitance. Using the formula,

$$C_s = Q / m \Delta V$$

A maximum specific capacitance of 344 F/g was obtained at a scan rate of 5mV/s. The particular capacitance values for different scan rates are presented in the Figure. 7(b) The specific capacitance values at scan rates of 5, 10, 25, and 50 mV-1 are 344, 273, 205, and 163 F/g, respectively, indicating a decrease in capacitance with increasing scan rate. At high scan rates, the diffusion process restricts OH-ion movement to the outer surface of the electrode, while at lower scan rates, the ions can intercalate with both surfaces

## 4. CONCLUSION

Nanocrystalline Co3O4 has been synthesised using a microwave method. The structural formation was confirmed through XRD measurements, which indicated an average grain size of 20 nm. Fourier-transform infrared (FT-IR) spectroscopy also revealed bonding interactions between oxygen and cobalt metal atoms. The electrical conductivity at elevated temperatures was analysed using impedance spectroscopy, which showed activation energies of 0.15 eV for the initial (extrinsic) properties and 0.74 eV for the final (intrinsic) properties. Interpreting the activation energy of Co3O4 ceramic semiconductors about grains, grain boundaries, and pores is rather complex. The dielectric constant and dielectric loss properties were also examined through impedance spectroscopy. High-temperature electrical resistivity was assessed using the van der Pauw method as a function of temperature, indicating that the resistivity of nanocrystalline Co3O4 decreases with increasing temperature from 350 K to 600 K, with the activation energy calculated from the Arrhenius plot being Ea = 0.23 eV. Field-emission scanning electron microscopy (FESEM) provided insights into the morphology of the nanoparticles. Additionally, cyclic voltammetry investigations emphasised the Faradic characteristics of the cobalt oxidation electrode, resulting in an optimal specific capacitance.

### Acknowledgement

The authors gratefully acknowledge Vels Institute of Science, Technology and Advanced Studies (VISTAS), Pallavaram, Chennai-600117, for providing Mrs. S. Sumathy, a part-time Research Scholar who has contributed to the execution of this research work. The authors express their sincere gratitude to Dr K. Ravichandran, Head of the Department of Nuclear Physics at the University of Madras, Tamil Nadu, India, for his invaluable guidance in the significant characterisation endeavours.

### Declaration of interests

The authors declare that they have no known competing financial interests or personal relationships that could have appeared to influence the work reported in this paper.

### Data availability

The authors confirm that the data supporting the findings of this study are available upon request.

### Declarations

### Conflict of interest

The authors have not disclosed any competing interests.

### Ethical approval

We confirm that the manuscript has been read and approved by all named authors and that no other persons satisfied the criteria for authorship but are not listed. We further confirm that we have all approved the authors' order in the manuscript.

**Author contributions**

**S. Sumathy:** Conceptualization, Methodology, Data curation, and Writing original draft; Methodology, Data curation; **Goparaju Savithri and Mohanraj M:** Data curation; **Dr M. Parthasarathy:** Methodology, Data curation, Investigation, Supervision and Validation.

## REFERENCES

[1] Synthesis and characterisation of cobalt oxide nanoparticles by thermal treatment process", Masoud Salavati-Niasari, Afsaneh Khansari Fatemeh Davar, *Inorganica Chimica Acta*, **362**, (2009) 4937–4942. https://doi.org/10.1016/j.ica.2009.07.023

[2] Science at the atomic scale", P. Ball, G. Li, *Nature*, **355** (1992), 761-766 http://dio.org/10.1038/355761a0.

[3] "Sustainable synthesis of cobalt and cobalt oxide nanoparticles and their catalytic and biomedical applications", Siavash Iravani, Rajender S. Varma, *Green Chemistry, 22,* (2020), 2643-2661. https://doi.org/10.1039/D0GC00885K

[4] "Synthesis and electrochemical properties of Co3O4 nanoparticles by hydrothermal method at different temperatures" Qiuyan Duan , Haiyan Chen, *Materials Science and Engineering,* **207,** (2017), 1-7. http://10.1088/1757-899X/207/1/012020

[5] "Precipitation method and characterization of cobalt oxide nanoparticles" D. Durai Manoharadoss Prabaharan, K. Sadaiyandi, M. Mahendran · Suresh Sagadevan, *Appl. Phys.* A, **123,** (2017), 1-6. https://doi.org/10.1007/s00339-017-0786-8

[6] "Study of influential factors in synthesis and characterization of cobalt oxide nanoparticles", Ghazaleh Allaedini, Abubakar Muhammad, *Journal of Nanostructure in Chemistry*, (2013),1-16. http://dio.org/10.1186/2193-8865-3-77

[7] "Facile fabrication of cobalt oxide nanograin-decorated reduced graphene oxide composite as an ultrasensitive platform for dopamine detection" Arshid Numan, Muhammad Mehmood, Shahid Fatin, Saiha Omar, K. Ramesh S. Ramesh. Sensors and Actuators B: Chemicals **238**, (2017),1043-1051 https://doi.org/10.1016/j.snb.2016.07.111

[8] "NiO nanoflakes: Effect of anions on the structural, optical, morphological and magnetic properties", R. Suresh, V. Ponnuswamy, C. Sankar, M. Manickam, S. Venkatesan, S. Perumal, *Journal of Magnetism and Magnetic Materials*, 425, (2017), 1-19.http://dx.doi.org/10.1016/j.jmmm.2017.05.069

[9] "Synthesis and characterization of cobalt oxide (Co3O4) nanoparticles", Rajan Lakra, Rahul Kumar, Dhirendra Nath Thatoi, Prasanta Kumar Sahoo, Ankur Soam, *Materials Today proceeding*, **41**,(2020), 269-271. https://doi.org/10.1016/j.matpr.2020.09.099

[10] "Impedance spectroscopy", J. Ross Macdonald, *Annals of Biomedical Engineering*, **20**, (1992), 289-305. https://jrossmacdonald.com/187ImpSpectroscopy

[11] "Impedance spectroscopy studies of Silver Doped Cadmium Sulphide Nanocrystallites" R. Sivanand, S. Chellammal, S. Manivannan, *Materials Science and Engineering,* 310, (2018),1-7. https://iopscience.iop.org/article/10.1088/1757-899X/310/1/012001/pdf

[12] "Fabrication, Mechanical properties, and Electrical Conductivity of $Co_3O_4$ Ceramics", Shinichi Sakamoto, Masaru Yoshinaka, *J. Am. ceramic. Soc*, **80**, (1997) 267–268. http://dx.doi.org/10.1111/j.1151-2916.1997.tb02824.x

[13] "Deficiency of $O_2$ molecules enhances ionic conductivity in Cr-doped O-Ce-O for solid oxide fuel cell applications", I. Mubeena Parveen, V. Asvini, G. Saravanan, K. Ravichandran, D.Kalaiselvi, *Ceramics International*, 45 (2019), 13127-13137. https://doi.org/10.1016/j.ceramint.2019.03.247

[14] "Microwave Assisted Synthesis of Co3O4 Nanoparticles for High-performance Supercapacitors**"** S. Vijayakumar, A. Kiruthika Ponnalagi, S. Nagamuthu and G. Muralidharan, *Electrochimica Acta*, *(*2013), 1-21. http://dx.doi.org/10.1016/j.electacta.2013.05.121

[15] "Tuning of Capacitance Behavior of NiO Using Anionic, Cationic, and Non-ionic Surfactants by Hydrothermal Synthesis", P. Justin, Sumanta Kumar Meher, and G. Ranga Rao, *J. Phys. Chem* **C,** 114, **(**2010), 5203–5210. https://pubs.acs.org/doi/abs/10.1021/jp9097155